Pressure-induced structural and electronic changes in α-AlH_3

J. Graetz,[1] S. Chaudhuri,[2] Y. Lee,[3] T. Vogt,[4] J. T. Muckerman,[2] and J. J. Reilly[1]
[1]*Department of Energy Sciences and Technology, Brookhaven National Laboratory, Upton, New York 11973, USA*
[2]*Department of Chemistry, Brookhaven National Laboratory, Upton, New York 11973, USA*
[3]*Department of Earth System Sciences, Yonsei University, Seoul 120749, South Korea*
[4]*USC NanoCenter and Department of Chemistry and Biochemistry, University of South Carolina, Columbia, South Carolina 29208, USA*
(Received 23 August 2006; revised manuscript received 31 October 2006; published 27 December 2006)

Pressure-induced structural, electronic, and thermodynamic changes in α-AlH_3 were investigated using synchrotron x-ray powder diffraction and density-functional theory. No first-order structural transitions were observed up to 7 GPa. However, increasing Bragg peak asymmetry with pressure suggests a possible monoclinic distortion at moderate pressures (1–7 GPa). The pressure-volume relationship was fit to the Birch-Murnaghan equation of state to give a bulk modulus of approximately 40 GPa. The reduced cell volume at high pressure is accommodated by octahedral tilting and a decrease of the Al-H bond distance. *Ab initio* calculations of the free energy indicate that hydrogenation becomes favorable at H_2 pressures above 0.7 GPa at 300 K. Electronic density of states calculations reveal a slight decrease in the band gap with pressure but no evidence of an insulator-to-metal transition predicted by previous high-pressure studies. Calculated Mulliken charges and bond populations suggest a mixed ionic and covalent Al-H bond at 1 atm with an increase in covalent character with pressure.

DOI: 10.1103/PhysRevB.74.214114 PACS number(s): 62.50.+p, 84.60.Ve, 71.20.−b, 61.10.Nz

I. INTRODUCTION

Aluminum hydride, AlH_3, is a unique binary hydride that is a promising hydrogen source for proton exchange membrane fuel cells and other applications. Despite a very low hydrogen solubility and the fact that aluminum is one of the most unlikely candidates to form a metal hydride, AlH_3 can be synthesized in seven different polymorphic structures (α, α', β, γ, δ, ϵ, and ζ) by simple organometallic methods.[1] On a volumetric basis, AlH_3 contains more than twice the hydrogen of liquid H_2 and it is one of only a few metal hydrides with a gravimetric hydrogen density that exceeds 10 wt. %. Most surprisingly, AlH_3 forms a stable, crystalline solid at room temperature despite an equilibrium hydrogen pressure greater than 0.3 GPa.[2,3]

The thermodynamics of α-AlH_3 have been investigated experimentally, using calorimetric techniques,[3–5] and computationally, using density-function theory (DFT).[6,7] These studies give a formation enthalpy of between −4.6 and −8.2 kJ/mol H_2. Using the more stable value for the formation enthalpy (−8.2 kJ/mol H_2) and an absolute entropy of 20 J/K mol H_2,[4] the lower bound on the H_2 fugacity necessary for hydride formation is 26 GPa (equivalent to 0.6 GPa H_2 pressure[8,9]) at room temperature. High-pressure experiments using H_2 as a pressure medium have demonstrated absorption in Al at 2.8 GPa at 573 K.[2,10] Although these values are in reasonable agreement, the structural and thermodynamic data of α-AlH_3 at high pressures remain incomplete. Pressure-induced structural and bonding changes are known to occur in a number of other metal hydrides, such as $LiAlH_4$ and $NaAlH_4$.[11] In this study, we investigate pressure-induced structural changes in α-AlH_3, which is comprised of corner shared AlH_6 octahedra. Similar to other investigations of distorted ReO_3 structures,[12,13] we use the rigid octahedral units as a basis for understanding structural changes in this system. Free-energy changes were calculated based on the experimentally determined structures (0–7 GPa) and calculated structures (15–100 GPa). Previous high-pressure structural studies of α-AlH_3, using energy dispersive x-ray powder diffraction,[14] and of α-AlD_3 using neutron powder diffraction,[15] measured unit-cell parameters and bulk moduli for these materials. Although neither study identifies any new powder-diffraction peaks that may be indicative of a pressure-induced phase change, the low resolution of the diffraction data limits the detection of more subtle structural changes.

Density-functional theory was used to calculate the change in free energy with pressure. We have calculated the electronic structure of monoclinic α-AlH_3 (space group $C2/c$) for the experimentally measured structures at pressures of 0–7 GPa and compared our findings with the DFT calculated values. High-pressure values quoted in this work represent the average stress applied to the system, which can be expressed as $\sigma_{\alpha\beta}$. This stress is related to the supercell volume (V_0) and the total energy (E_{tot}) in the following way:

$$\sigma_{\alpha\beta} = \frac{1}{V_0}\frac{\partial E_{\text{tot}}}{\partial \epsilon_{\alpha\beta}}, \tag{1}$$

where $\epsilon_{\alpha\beta}$ is the component of the strain tensor.[16,17] This method has shown good agreement with the experimental values for unit-cell parameters and the bulk modulus. We extend the calculation of the equilibrium structure to a pressure range of 15–100 GPa where the experimental values are not available. This allows us to investigate the possibility of an insulator-to-metal transition, which is predicted to occur between 50 and 100 GPa.[2,18]

The Al-H bonding in AlH_3 is characterized in the literature as both covalent[19] and ionic.[15,20] Both descriptions are reasonable since Al-H bonding in other environments, such as the complex metal hydrides (e.g., $NaAlH_4$), is predominately covalent, while M-H bonding in most binary metal

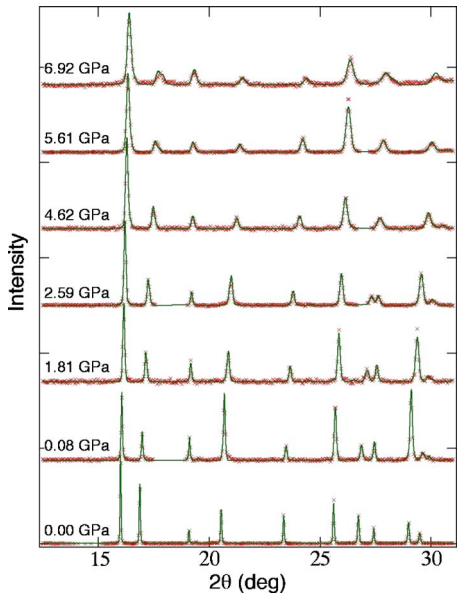

FIG. 1. (Color online) X-ray powder-diffraction patterns from α-AlH_3 at pressures of 0.0–6.9 GPa showing observed data (+) and Lebail profile fits (solid line) using a monoclinic unit cell ($C2/c$).

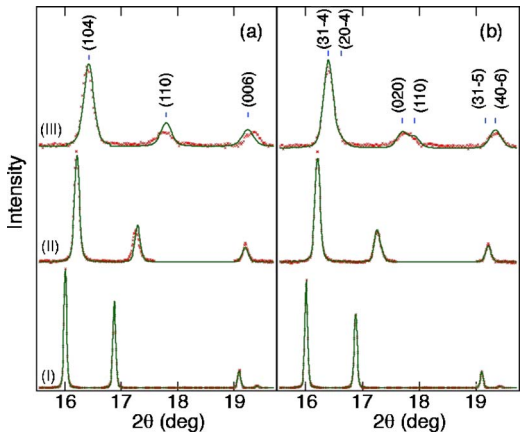

FIG. 2. (Color online) X-ray powder-diffraction patterns (+) from α-AlH_3 at (I) 0.0 GPa, (II) 2.6 GPa, and (III) 6.9 GPa with Lebail profile fits (solid line) using space groups (a) $R\bar{3}c$ (b) $C2/c$. The respective Rwp (Rp) values were 2.8% (2.3%), 2.3% (1.7%), and 4.7% (3.8%) using space group $C2/c$ and 3.2% (2.5%), 3.6% (2.3%), 6.4% (5.0%) using $R\bar{3}c$. The diffraction peaks are indexed according to the space group used in the profile fit.

hydrides (e.g., NaH) is strongly ionic. However, given a purely ionic model, AlH_3 would only exist in a cubic phase where the Al^{3+}-Al^{3+} repulsion along all three directions could be shielded by a H^- ion. A more accurate description is that the Al-H bond is highly polarizable and has contributions from both covalent and ionic wave functions, which are nonorthogonal in this system. As a result, multiple polymorphs of AlH_3 exist (the most stable of which is the α phase[1]) contributing to a complex potential-energy surface with multiple metastable minima. In this study, we use the Mulliken charges combined with a bond population picture to quantify the nature of the bonding in α-AlH_3 at pressures up to 100 GPa.

II. EXPERIMENT

Samples of α-AlH_3 powder were synthesized by the Dow Chemical Co. using an ethereal reaction of $LiAlH_4$ and $AlCl_3$ as described by Brower *et al.*[1] Previous elemental analyses of the Dow material revealed contaminants of Al_2O_3 (2%), $LiAlH_4$ (1%), and $AlCl_3$ (1%).[4] The material used in this study has a slightly lower sample purity (by about 3%),[21] which is attributed to a small amount of decomposition over 25 years. α-AlH_3 does not form a solid solution (e.g., AlH_x where $0<x<3$)[3] and therefore a small amount of decomposition may yield higher concentrations of Al and Al_2O_3, but will not affect the structure of α-AlH_3. Although the structure of Al_2O_3 is also $R\bar{3}c$, the lattice parameters are ~10% larger at 1 atm and thus easily distinguishable from α-AlH_3.

The large crystallites (50–100 μm) of α-AlH_3 were crushed with a mortar and pestle to reduce the particle size for better powder averaging. Structural studies were performed using synchrotron x-ray diffraction (XRD) on beamline X7A at the National Synchrotron Light Source of Brookhaven National Laboratory. A monochromatic beam was selected using a channel-cut Si(111) monochromator and a gas-proportional position-sensitive detector (PSD), gated at the Kr-escape peak, was used for high angular resolution ($\Delta d/d \sim 10^{-3}$).[22]

A modified Merrill-Bassett-type diamond-anvil cell (DAC) was used for high-pressure measurements and hydrostatic pressure conditions were achieved using Fluorinert as a pressure medium. Several small ruby chips were loaded with the sample in the DAC. The sample pressure was measured from the position of the ruby $R1$ emission line with an uncertainty of ±0.1 GPa. The high-pressure diffraction data was acquired between 10° and 35° in 2θ using an x-ray wavelength of $\lambda=0.6541$ Å. A powder sample of α-AlH_3 was also run at ambient pressure in a spinning glass capillary tube (0.3 mm) sealed under Ar gas. The 1 atm diffraction data was acquired between 10° and 60° in 2θ with a wavelength of $\lambda=0.6985$ Å. (The 2θ scale for the 1-atm pattern was ajusted to compensate for the small wavelength difference and match the high-pressure patterns in Figs. 1 and 2.) Diffraction peaks from the sample holder and the pressure gasket were removed from all patterns. Analysis of the diffraction data was performed using GSAS with EXPGUI.[23,24] The refinements were made over the entire 2θ range except for the regions near 18.2° in 2θ, where broad diffraction peaks from the stainless-steel gasket appeared.

Kohn-Sham density-functional theory within the generalized gradient approximation (GGA) was used to calculate the stability of α-AlH_3 and the structural changes with pressure. The starting structure was determined from the synchrotron diffraction data and it was optimized using the quasi-Newtonian Broyden-Fletcher-Goldfarb-Shanno (BFGS) algorithm. The Brillouin-zone sampling was performed using a Monkhorst-Pack grid of $10\times6\times7$ with a total of 105 k points. Ultrasoft plane-wave pseudopotentials as implemented in the program CASTEP were used in this work to

TABLE I. High-pressure structural parameters for α-AlH_3. The unit-cell parameters (a, b, c, β, and V) were determined from Lebail fits using the space group $C2/c$. The experimentally measured lattice constants were used to calculate the Al-H bond distances and the free-energy change ΔE from DFT. The values given for $P \geqslant 15$ GPa (*) were determined from calculated lattice constants.

Pressure (GPa)	Lattice constants a, b, c	β (*)	V (Å^3)	Al-H length (Å)	ΔE (kJ/mol AlH_3)
0.00	8.2958(1), 4.4583(1) 11.8303(1)	161.96(1)	135.55(13)	1.703	0.0000
1.81	8.2550(5), 4.3792(3), 11.7893(7)	162.08(1)	131.10(13)	1.697	0.9284
2.59	8.2403(3), 4.3469(2), 11.7698(5)	162.16(1)	129.17(10)	1.697	1.573
4.62	8.1987(8), 4.2931(5), 11.7009(15)	162.57(1)	123.34(14)	1.688	4.344
5.61	8.1690(5), 4.2631(4), 11.6748(8)	162.71(1)	120.83(10)	1.687	6.230
6.92	8.1584(14), 4.2372(9), 11.6482(25)	162.84(1)	118.81(15)	1.684	7.880
15*	7.7947, 4.0056, 11.1696	162.75	103.39	1.650	29.86
25*	7.5888, 3.8630, 10.8841	162.90	93.801	1.626	58.06
50*	7.2274, 3.6598, 10.3663	162.71	80.106	1.581	132.6
100*	6.7388, 3.4468, 9.6582	162.81	66.285	1.522	284.2

describe the core electrons in the periodic DFT calculations.[25] The plane-wave basis set cutoff of 240 eV was found to be adequate for well-converged total energies. We tested PBE and RPBE exchange-correlation functionals and most of the calculations presented here use RPBE functionals.[26,27] Isotropic pressures of 0–100 GPa were applied to the unit cell to calculate changes in energy, volume, and atomic positions. Band structures and density of states (DOS) were calculated at a Fermi energy convergence tolerance of 0.533×10^{-7} eV/atom and included 18 extra unoccupied bands. A Mulliken population analysis[28] was performed to gain insight into the nature of bonding and redistribution of charge with pressure. Mulliken charges and bond populations were obtained from the overlap and density matrices determined from eigenstates calculated using a plane-wave basis and projected onto Bloch functions formed from a linear combination of atomic orbitals (LCAO) basis.

III. RESULTS

Synchrotron x-ray-diffraction spectra were acquired at 1 atm in a glass capillary and under hydrostatic pressure up to 6.9 GPa in a DAC. A full Rietveld analysis of the 1-atm pattern revealed a good fit for the hexagonal space group $R\bar{3}c$ [a=4.4553(1) Å, c=11.8306(1) Å, and V =203.371(4) Å^3] with Rwp=3.2% and Rp=2.5%. Diffraction patterns acquired at high pressures 0.8–6.9 GPa and the corresponding Lebail fits are shown in Fig. 1. The powder-diffraction peaks broaden and shift to higher angles with increasing pressure, but there is no indication of new peak formation resulting from a first-order structural transition. However, a slight Bragg peak asymmetry was observed at high pressure, possibly due to a monoclinic distortion. The high-pressure diffraction patterns were fit with the hexagonal space group, $R\bar{3}c$, and a monoclinic subgroup, $C2/c$. Fitting in the monoclinic subgroup $C2/c$ gave the most satisfactory result with regard to the agreement indices, as shown in Fig. 2. Rietveld fits to the 1-atm pattern using $C2/c$ gave reliability factors similar to those obtained with $R\bar{3}c$ (Rwp=2.8% and Rp=2.3%).

The structural parameters for α-AlH_3 under pressure are listed in Table I. The unit-cell parameters (a, b, c, β, and V) were determined from Rietveld and Lebail fits using a monoclinic ($C2/c$) space group. The Al-H bond distances were calculated from experimentally measured lattice constants using DFT (T=0 K). Actual bond distances may be slightly larger due to thermal vibrations at finite temperature. The free-energy change ΔE was calculated with respect to the 0 -GPa structure using the experimental lattice parameters for α-AlH_3. The normalized lattice constants (a, b, c, β, and V) are plotted in Fig. 3. The calculated error bars, determined from the Lebail fits, were typically larger at higher pressures but in all cases smaller than the markers used in the figure. The normalized cell volume ($x \equiv V/V_0$) was fit to the third-

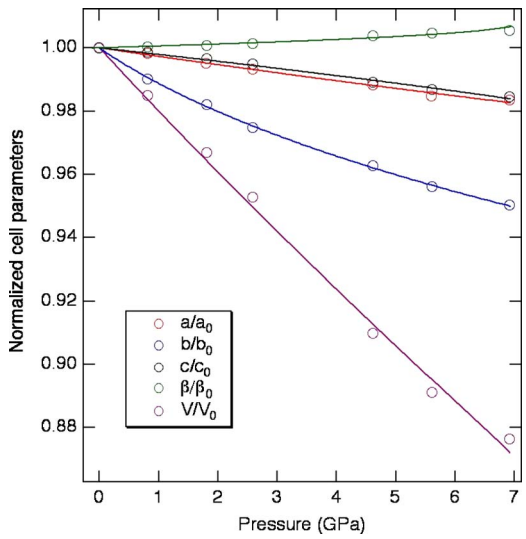

FIG. 3. (Color online) Normalized cell parameters a, b, c, β, and V (cell volume) for α-AlH_3 determined from Lebail fits of the powder-diffraction data.

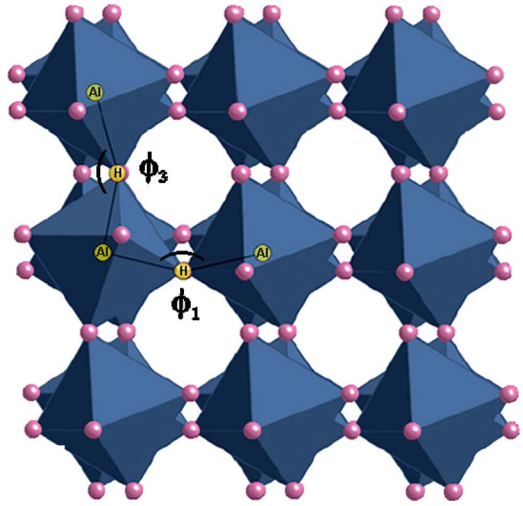

FIG. 4. (Color online) AlH_6 octahedra in α-AlH_3 showing the different Al-H-Al bond angles ϕ_1 and ϕ_3 (ϕ_2 describes the angle of the A-H-Al bond going into the page and is equivalent to ϕ_1).

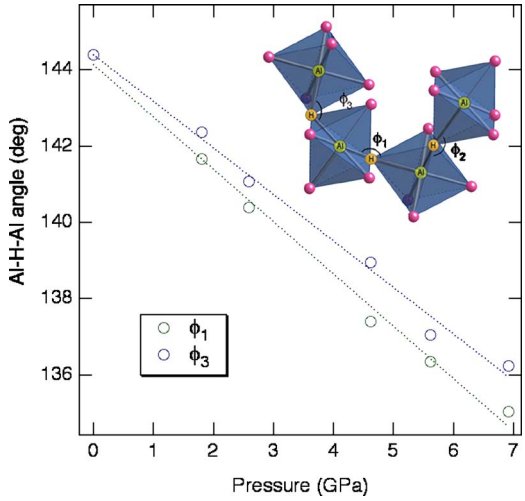

FIG. 5. (Color online) Change in Al-H-Al bond angles (ϕ_1 and ϕ_3) with pressure. The inset shows the three different octahedral angles ($\phi_1=\phi_2$) in AlH_3.

order isothermal Birch-Murnaghan equation of state (EOS):[29]

$$P(V) = \frac{3}{2}B_0(x^{-7/3} - x^{-5/3})\left[1 + \frac{3}{4}(B_0' - 4)(x^{-2/3} - 1)\right]. \quad (2)$$

The EOS fit to the normalized experimental volume gives the bulk modulus at zero pressure, $B_0=49\pm4$ GPa, and the pressure derivative of the bulk modulus, $B_0'=1\pm1$. In this case (experimental volumes only) the value for B_0' is unusually small and likely overestimates B_0. More reasonable bulk modulus constants $B_0=40\pm2$ GPa and $B_0'=3.1\pm0.2$, are obtained when the EOS is fit to a data set that includes the calculated volumes ($\leqslant$25 GPa). In both cases the values are similar to those measured by Baranowski *et al.* (B_0 =47.9 GPa and $B_0'=3.3$).[14]

A structural diagram showing tilted AlH_6 octahedra in α -AlH_3 is shown in Fig. 4. The tilting system for $R\bar{3}c$ is denoted as $a^-a^-a^-$ using the notation introduced by Glazer[30] for perovskites. In this scheme, the tilt systems are defined along the three orthogonal axes a, b, and c, which define the directions of the original cubic cell (denoted as $a^0a^0a^0$). The superscripts (+, 0, or −) indicate the sense of the tilt in successive layers, + and − indicating in-phase (+) or out-of-phase (−) tilts. The letters a, b, and c are used to indicate the relative sizes of the tilts in the three orthogonal directions. Our high-pressure structural results suggest a tilting scheme of $a^-b^-c^-$ indicating that the magnitude of the out-of-phase octahedral rotation is different along each of the three Glazer axes. The octahedral tilting can also be defined in terms of the characteristic Al-H-Al bond angles ϕ_1, ϕ_2, and ϕ_3 that correspond to the relative orientations of corner-shared AlH_6 octahedral units in three perpendicular directions as shown in Fig. 4. In α-AlH_3 the bond angles ϕ_1 ($\phi_1=\phi_2$) and ϕ_3 change continuously with pressure (up to 6.9 GPa) as shown in Fig. 5.

The results presented in Table I indicate a ~51% reduction in the cell volume between 0 and 100 GPa. This decrease in volume under applied pressure is achieved by increasing the tilting (changes in $\phi_{1,2}$ and ϕ_3) and compression of the AlH_6 octahedra. The Al-H bond distance is reduced from 1.703 Å at 0 GPa to 1.522 Å at 100 GPa. The expected Al-H bond distance based on ionic radii (Al^{3+} and H^-) is 2.08 Å (Refs. 31 and 32) and 1.56 Å based on covalent radii,[32] suggesting a trend towards increasing covalent character with pressure. The equilibrium bond length, and the AlH_6 octahedra as a whole, undergo significant compression. It is important to note that at a given pressure the calculated equilibrium bond distances are the same for all Al-H bonds (±0.004 Å). Therefore although there is a difference in bond angles (Fig. 5) there is no pronounced distortion of the AlH_6 octahedra at high pressure (up to 100 GPa).

The change in free energy with decreasing cell volume (increasing pressure) is plotted in Fig. 6. The inset shows how the room-temperature equilibrium H_2 fugacity f_{H_2} is affected by the applied pressure. f_{H_2} is the minimum H_2 fugacity necessary for hydrogenation of Al metal to form AlH_3. f_{H_2} was calculated from the change in free energy ΔE listed in Table I and the Gibbs free energy at 1 atm, ΔG_0:

$$f_{H_2}(V) = \exp\left(\frac{\Delta G_0 + \Delta E(V)}{RT}\right), \quad (3)$$

where R is the universal gas constant. The equilibrium fugacity curve was calculated form the Gibbs free energy measured calorimetrically $\Delta G_0=31.0$ kJ/mol H_2,[4] and the fugacity versus pressure relationship for H_2 was determined from pressure-volume-temperature (PVT) data.[8,9]

The electronic DOS calculated from DFT at pressures of 0, 50, and 100 GPa are shown in Fig. 7. The occupied states below the Fermi level (E_F) are dominated by Al 3p, 3s and H 1s states. The DOS widens considerably (Fig. 7) both below and above E_F with increasing pressure. The initial valence-band width of 10.5 eV increases to approximately 13.0 and 15.0 eV at 50 and 100 GPa, respectively. As a result, there is a net increase in the overlap between the Al 3p and H 1s

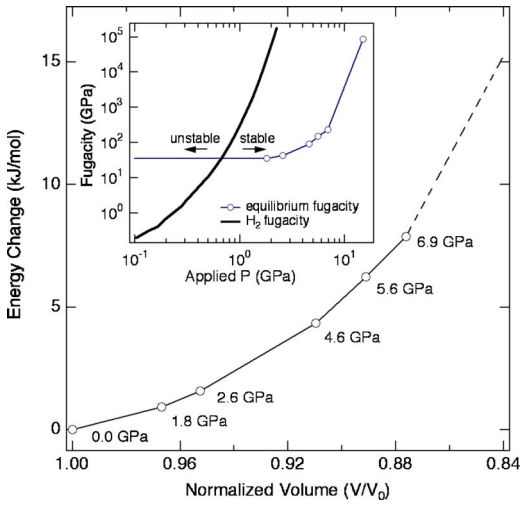

FIG. 6. (Color online) Calculated free-energy change based on experimental lattice parameters for pressures 0.0–6.9 GPa (solid line). The dashed line connects the experimental values with the calculated values at 15 GPa. The inset shows how the equilibrium H_2 fugacity (the minimum H_2 fugacity necessary for hydride formation [Eq. (3)] at 300 K changes with applied pressure based on the calculated ΔE and the Gibbs free energy from calorimetric studies (Ref. 4). The thick line represents the fugacity versus pressure relationship for gaseous H_2 (Refs. 8 and 9) and denotes an AlH_3 stability boundary.

states, although the bonding is still predominately ionic. The greater octahedral tilting increases the repulsion between the Al $3p$ states belonging to adjacent AlH_6 octahedra and broadens the bands with decreasing Al-H-Al bond angles. Although an insulator-to-metal transition is a reasonable possibility with increasing repulsion, the widening of the DOS is nearly isotropic around E_F resulting in a band gap that is essentially invariant with pressure. The Mulliken charges and overlap populations calculated at 0, 7, and 100 GPa are shown in supplementary Tables 1–3.[33]

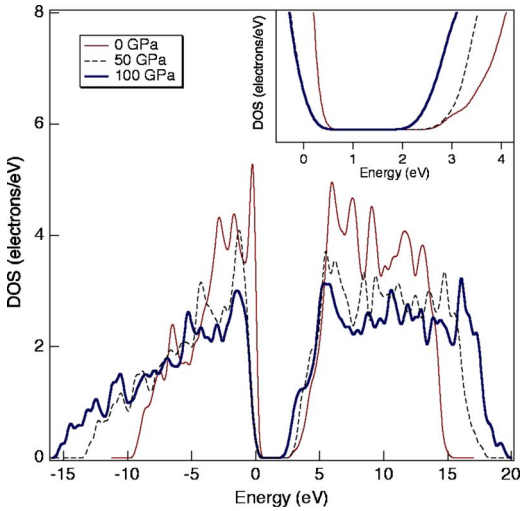

FIG. 7. (Color online) Electronic density of states for α-AlH_3 at 0, 50, and 100 GPa showing an overall widening of the bands with increasing pressure. The band gap increases slightly from 2.2 eV at 0 to 2.5 GPa at 50 GPa and then decreases to 1.9 eV at 100 GPa.

IV. DISCUSSION

A. Crystallographic structure

The powder-diffraction peaks of α-AlH_3 exhibit a slight anisotropy with increasing pressure (Fig. 2). There are a number of possible origins for the Bragg peak asymmetry and anisotropy, including instrumentation artifacts, anisotropic strain broadening, accumulation of stacking faults, or a monoclinic distortion of the unit cell. An instrumentation problem, such as axial divergence asymmetry, would occur exclusively on the low angle side of the powder-diffraction peaks and is therefore unlikely since the new shoulder often appears on the high-angle side (e.g., ~16.5°). Stacking fault accumulation is also unlikely due to the polymeric nature of the structure, which consists of a network of corner connected octahedra. Therefore the progressive Bragg peak broadening and splitting is most likely attributed to some sort of crystal deformation either on the atomic or macroscopic scale. This is also supported by the divergence of the Al-H-Al bonding angles ($\phi_{1,2}$ and ϕ_3) shown in Fig. 5. This anisotropy could be attributed to the Flourinert pressure medium, which transforms to a glass under pressure and may exhort increasing anisotropic strain as the pressure is increased. However, there were no such indications based on the ruby fluorescence signal and anisotropy terms introduced in the refinements did not lead to any meaningful improvement in the fit quality. Therefore unit-cell refinements used a monoclinic subgroup ($C2/c$) to accommodate all possible structural deformations and give the most realistic phase compressibility. Although a monoclinic distortion was not identified by previous high-pressure experiments, this may be due to limited 2θ resolution in these studies.[14,15] Our refinements suggest the possibility of a slight monoclinic distortion at moderate pressures (1–7 GPa). However, it is unlikely that the unit cell deviates significantly from the $R\bar{3}c$ space group at higher pressure, since no new powder-diffraction peaks were observed by Baranowski *et al.* at pressures up to 35 GPa,[14] and Jephcoat *et al.* up to 54 GPa.[18]

B. Thermodynamics

Despite numerous thermodynamic measurements on α-AlH_3, little is know about the structural and thermodynamic properties of this material under high pressure. Recent DFT calculations have identified two structures of AlH_3 (cubic and orthorhombic) that are predicted to be more stable than the known hexagonal structure (α-AlH_3).[7] A more stable AlH_3 phase, one that could be formed from the elements under moderate hydrogenation pressures, would have significant implications for energy storage. However, the possibility of a more stable high-pressure phase can easily be dismissed from the powder-diffraction data of Fig. 1, which clearly shows that no pressure-driven structural transitions occur at pressures up to approximately 7 GPa. The calculated free energies of α-AlH_3 under high pressure (Fig. 6) suggest an overall destabilization of the hydride due to the lattice distortion. The inset of Fig. 6 reveals that the fugacity necessary for hydride formation (equilibrium fugacity) increases rapidly with applied pressure. If H_2 is treated strictly

as an ideal gas, these results suggest that α-AlH_3 is thermodynamically unstable at all H_2 pressures and high-pressure hydrogenation of Al should be impossible. However, H_2 deviates from the ideal gas behavior at high pressures and the thermodynamic activity of H_2 is considerably higher than expected from an ideal gas as shown in the inset of Fig. 6 (H_2 fugacity).[8,9] The ratio of fugacity to pressure for H_2 gas is 1 at 0.1 MPa (1 atm), ~2 at 0.1 GPa, and ~300 at 1 GPa. Therefore hydrogenation occurs at much lower pressures than predicted from the ideal gas state equation. The minimum H_2 pressure necessary for hydride formation (α-AlH_3) at 300 K is 0.7 GPa ($f_{H_2} \approx 50$ GPa), which is in reasonable agreement with high-pressure hydrogenation experiments.[2,10]

C. Electronic structure

Pressure-induced insulator-to-metal transitions are known to occur in a number of metal hydrides.[34] An insulator-to-metal transition is expected in α-AlH_3 when the effective volume of the H atom in AlH_3 is reduced to the volume of H in the transition-metal hydrides (~3 Å^3). This crossover is predicted to occur between 50 and 100 GPa.[14,18] Such a transition would be characterized by an enhanced electrical conductivity, a change in the optical properties [loss of transparency is observed between 43 and 47 GPa (Ref. 18)] and an increase in H mobility from the breakup of Al-H-Al bridging bonds.[14] The effective H volume V_H determined from our high-pressure x-ray data and DFT results (up to 100 GPa) suggest that $V_H = 3$ Å^3 at approximately 45 GPa (Fig. 8). This value is in agreement with Baranowski *et al.*,[14] but is approximately 45 GPa less than the crossover pressure predicted by Jephcoat and Besedin based on extrapolated high-pressure data.[18] Therefore we have calculated the total electronic density of states up to 100 GPa with 18 empty bands above the Fermi level. The DOS calculated for the 1-atm experimental structure is similar to the results for the hexagonal AlH_3 phase calculated by Ke *et al.*[7] and Aguayo *et al.*[20] With increasing pressure, the bands above and below the Fermi edge widen, resulting in a slight decrease in the band gap at 100 GPa (Fig. 7). There is no evidence of an insulator-to-metal transition at $V_H = 3$ Å^3. The possibility of forming a high-pressure phase where mobile H atoms exist in a solid solution within the Al matrix (as proposed by Baranowski *et al.*[14]) is unlikely.

At ambient pressure the molar volume of α-AlH_3 is twice that of Al metal and therefore, the Al-H bonds are expected to be of a mixed ionic and covalent character.[14,35] This is supported by the calculated Mulliken charges at 0 GPa, which are +1.32 and −0.44 for aluminum and hydrogen, respectively. The bond population analysis in the rhombohedral space group shows that the six bonds in the AlH_6 octahedra do not have equivalent electronic structure. Although the octahedron as a whole is not distorted, the population of one pair of Al-H bonds, 0.53, is significantly different from the population of the other two pairs, 0.42 and 0.43 (see supplementary Table 1).[33] The populations along the direction of the shared corner of the octahedra, i.e., along any Al-H-Al zigzag chain, are equivalent. Based on volumetric considerations, the character of the Al-H bond is expected to become progressively more ionic (similar to the transition metal hydrides) with increasing pressure. However, the calculated Mulliken charges and bond populations at 7 GPa suggest a trend toward increasing covalent overlap in this predominantly ionic solid. At this pressure the magnitude of the charges on the Al and H ions are reduced (+1.28 and −0.41), while the bond populations along the three unique directions increases to 0.57, 0.46, and 0.44, respectively (see supplementary Table 2).[33] The trend of decreasing charge and increasing bond population was observed up to 100 GPa, where the bond populations are 0.77, 0.66, and 0.51 and the charges on the Al and H ions are 1.15 and −0.38, respectively (see supplementary Table 3).[33] As the atoms are confined to a progressively smaller space the overlap between the Al 3*p* and H 1*s* bands increases, resulting in a small, but noteworthy covalent contribution to the Al-H bond.

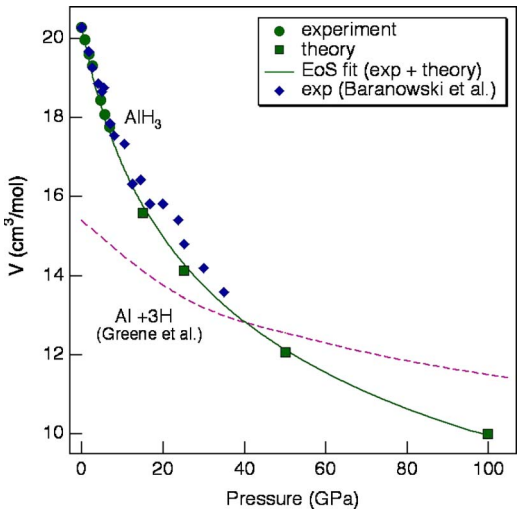

FIG. 8. (Color online) Molar volume of AlH_3 determined from high-pressure diffraction (●), DFT calculations (■), and the high-pressure study of Baranowski *et al.* (◆) (Ref. 14). Also shown is the Birch-Murnaghan EOS fit (0–100 GPa) and the pressure and volume curve for the sum of the volumes from Al metal (Ref. 36) and 3-H atoms ($V_H = 3$ Å^3 = 1.8 cm^3/mol H). The H volume is assumed invariant with pressure.

V. CONCLUSION

A high-pressure investigation of α-AlH_3 revealed no indication of a first-order structural transition up to 7 GPa and up to 100 GPa based on calculated structures. A slight Bragg peak asymmetry observed at moderate pressures (1–7 GPa) suggests a possible monoclinic distortion of the unit cell. The cell volume decreases by ~13% between 0 and 7 GPa (experimental) and by ~51% between 0 and 100 GPa (calculated). This change is compensated by AlH_6 octahedral tilting and a shrinking of the Al-H bond distance. The

calculated free-energy change suggests that the hydride becomes stabilized at H_2 pressures greater than 0.7 GPa at 300 K. The effective H volume in α-AlH_3 is equivalent to that of the transition-metal hydrides (~ 3 Å^3) at a pressure of 45 GPa. However, analysis of the electronic DOS up to 100 GPa reveals no evidence of an insulator-to-metal transition. Electronic structure calculations also reveal a mixed ionic and covalent Al-H bond at ambient pressure with increasing covalent character with pressure.

ACKNOWLEDGMENTS

This paper has been authored by Brookhaven Science Associates, LLC under Contract No. DE-AC02-98CH1-886 with the U.S. Department of Energy. This work, including research carried out at the NSLS (beamline X7A), was supported by the Lab Directed Research and Development Program at Brookhaven.

[1] F. M. Brower, N. E. Matzek, P. F. Reigler, H. W. Rinn, C. B. Roberts, D. L. Schmidt, J. A. Snover, and K. Terada, J. Am. Chem. Soc. **98**, 2450 (1976).
[2] B. Baranowski and M. Tkacz, Z. Phys. Chem., Neue Folge **135**, 27 (1983).
[3] J. J. Graetz and J. Reilly, J. Alloys Compd. **424**, 262 (2006).
[4] G. C. Sinke, L. C. Walker, F. L. Oetting, and D. R. Stull, J. Chem. Phys. **47**, 2759 (1967).
[5] S. Orimo, Y. Nakamori, T. Kato, C. Brown, and C. M. Jensen, Appl. Phys. A: Mater. Sci. Process. **83**, 5 (2006).
[6] C. Wolverton, V. Ozolins, and M. Asta, Phys. Rev. B **69**, 144109 (2004).
[7] X. Ke, A. Kuwabara, and I. Tanaka, Phys. Rev. B **71**, 184107 (2005).
[8] W. de Graff, Ph.D. thesis, University of Amsterdam, Amsterdam (1960).
[9] B. Baranowski, Ber. Bunsenges. Phys. Chem. **76**, 714 (1972).
[10] A. K. Konovalov and B. M. Bulychev, Inorg. Chem. **34**, 172 (1995).
[11] P. Ravindran, P. Vajeeston, H. Fjellvag, and A. Kjekshus, Comput. Mater. Sci. **30**, 349 (2004).
[12] S. Chaudhuri, P. J. Chupas, M. Wilson, P. Madden, and C. P. Grey, J. Phys. Chem. B **108**, 3437 (2004).
[13] P. B. Allen, Y. R. Chen, S. Chaudhuri, and C. P. Grey, Phys. Rev. B **73**, 172102 (2006).
[14] B. Baranowski, H. D. Hochheimer, K. Strossner, and W. Honle, J. Less-Common Met. **113**, 341 (1985).
[15] I. N. Goncharenko, V. P. Glazkov, A. V. Irodova, and V. A. Somenkov, Physica B **174**, 117 (1991).
[16] V. B. Deyirmenjian, V. Heine, M. C. Payne, V. Milman, R. M. Lynden-Bell, and M. W. Finnis, Phys. Rev. B **52**, 15191 (1995).
[17] O. H. Nielsen and R. M. Martin, Phys. Rev. B **32**, 3792 (1985).
[18] A. P. Jephcoat and S. P. Besedin, ESRF Report, exp. HC104, 1995.
[19] B. Siegel, G. Libowitz, G. G. Libowitz, W. M. Mueller, J. P. Blackledge, and G. G. Libowitz, in *Metal Hydrides*, edited by W. M. Mueller, J. P. Blackledge, and G. G. Libowitz (Academic, New York, 1968), p. 545.
[20] A. Aguayo and D. J. Singh, Phys. Rev. B **69**, 155103 (2004).
[21] G. Sandrock, J. Reilly, J. Graetz, W. M. Zhou, J. Johnson, and J. Wegrzyn, Appl. Phys. A: Mater. Sci. Process. **80**, 687 (2005).
[22] G. C. Smith, Synchrotron Radiat. News **4**, 24 (1991).
[23] A. C. Larson and R. B. Vondreele, GSAS, General Structure Analysis System. Report No. LAUR 86–745, Los Alomos National Lab, New Mexico (1986).
[24] B. H. Toby, J. Appl. Crystallogr. **34**, 210 (2001).
[25] M. D. Segall, P. J. D. Lindan, M. J. Probert, C. J. Pickard, P. J. Hasnip, S. J. Clark, and M. C. Payne, J. Phys.: Condens. Matter **14**, 2717 (2002).
[26] J. P. Perdew, K. Burke, and M. Ernzerhof, Phys. Rev. Lett. **77**, 3865 (1996).
[27] B. Hammer, L. B. Hansen, and J. K. Norskov, Phys. Rev. B **59**, 7413 (1999).
[28] R. S. Mulliken, J. Chem. Phys. **23**, 1833 (1955).
[29] F. Birch, Phys. Rev. **71**, 809 (1947).
[30] A. M. Glazer, Acta Crystallogr., Sect. B: Struct. Crystallogr. Cryst. Chem. **28**, 3384 (1972).
[31] R. D. Shannon, Acta Crystallogr., Sect. A: Cryst. Phys., Diffr., Theor. Gen. Crystallogr. **32**, 751 (1976).
[32] *Lange's Handbook of Chemistry*, 15th Edition, edited by J. A. Dean (McGraw-Hill, New York 1999), pp. 4.31–4.35.
[33] See EPAPS Document No. E-PRBMDO-74-072645 for supplementary tables. For more information on EPAPS, see http://www.aip.org/pubservs/epaps.html
[34] C. M. Araujo, A. F. da Silva, and R. Ahuja, Phys. Status Solidi B **241**, 3219 (2004).
[35] J. W. Turley and H. W. Rinn, Inorg. Chem. **8**, 18 (1969).
[36] R. G. Greene, H. Luo, and A. L. Ruoff, Phys. Rev. Lett. **73**, 2075 (1994).